This is the peer reviewed version of the following article:

Hernández-López L., Martínez-Esaín J., Carné-Sánchez A., Grancha T., Faraudo J., Maspoch D.. Steric Hindrance in Metal Coordination Drives the Separation of Pyridine Regioisomers Using Rhodium(II)-Based Metal–Organic Polyhedra. Angewandte Chemie - International Edition, (2021). 60. : 11406 - . 10.1002/anie.202100091,

which has been published in final form at https://dx.doi.org/10.1002/anie.202100091. This article may be used for non-commercial purposes in accordance with Wiley Terms and Conditions for Use of Self-Archived Versions.

Steric Hindrance in Metal Coordination Drives the Separation of Pyridine Regioisomers Using Rhodium(II)-Based Metal–Organic Polyhedra

Laura Hernández-López,[a] Jordi Martínez-Esaín,[a] Arnau Carné-Sánchez,*[a] Thais Grancha,[a] Jordi Faraudo, [b] and Daniel Maspoch *[a][c]

[a] L. Hernández-López, J. Martínez-Esaín, Dr. A. Carné-Sánchez, Dr. T. Grancha, Prof. Dr. D. Maspoch.
Catalan Institute of Nanoscience and Nanotechnology (ICN2), CSIC and The Barcelona Institute of Science and Technology, Campus UAB, Bellaterra, 08193 Barcelona, Spain.
E-mail: Arnau.carne@icn2.cat, daniel.maspoch@icn2.cat
[b] Dr. J. Faraudo.
Institut de Ciència de Materials de Barcelona (ICMAB-CSIC), E-08193 Bellaterra, Spain
[c] Prof. Dr. D. Maspoch.
ICREA, Pg. Lluís Companys 23, 08010 Barcelona, Spain

Supporting information for this article is given via a link at the end of the document.

Abstract: The physicochemical similarity of isomers makes their chemical separation through conventional techniques energy intensive. Herein, we report that, instead of using traditional encapsulation-driven processes, steric hindrance in metal coordination on the outer surface of Rh(II)-Based Metal Organic Polyhedra (Rh-MOPs) can be used to separate pyridine-based regioisomers via liquid-liquid extraction. Through molecular dynamics simulations and wet experiments, we discovered that the capacity of pyridines to coordinatively bind to Rh-MOPs is determined by the positions of the pyridine substituents relative to the pyridine nitrogen and is influenced by steric hindrance. Thus, we exploited the differential solubility of bound and non-bound pyridine regioisomers to engineer liquid-liquid self-sorting systems. As proof-of-concept, we separated four different equimolecular mixtures of regioisomers, including a mixture of the industrially-relevant compounds 2-chloropyridine and 3-chloropyridine, isolating highly pure compounds in all cases.

Introduction

Chemical separations are crucial but problematic steps in industrial purification. They are energy intensive and expensive, especially for mixtures of chemicals with similar solubility, boiling point, and/or molecular size or shape.[1] An especially challenging case is the separation of isomeric mixtures, for which common methods such as distillation, extraction and chromatography are often insufficient.[2] Archetypical regioisomers that are difficult to separate include aliphatic compounds,[3] aromatic compounds,[4] and heterocycles[5] such as functionalised pyridines.[6] These include pyridine derivatives that are extensively used in the pharmaceuticals and fine chemicals sectors, whose production often leads to mixtures of regioisomers that must be separated.[7] Such is the case with 2-chloropyridine (2-ClPy) and 3-chloropyridine (3-ClPy), common synthetic building blocks for drugs and pesticides.[8]

Great effort has been focused on the development of new, less-energy-intensive methods for chemical separation. One example is adsorption of the compounds to be separated by distinct porous materials.[9] Indeed, inorganic zeolites,[10] covalent organic frameworks (COFs)[11] and metal-organic frameworks (MOFs)[12,13] have all been used as selective adsorbents, thanks to the facility with which their cavities can be rationally designed for selective recognition of target isomers. However, crystalline porous solids are

employed in heterogeneous systems that often require vaporisation of molecules and subsequent activation of the adsorbent, drawing on additional energy resources.[4] An alternative type of porous materials to these is discrete molecules with defined cavities, such as macrocycles,[14,15] porous organic cages[16] and metal-organic cages.[17–20] These materials are amenable to selective host-guest recognition in liquid-based separation methodologies (*e.g.* liquid-liquid extraction), which are known in industry for requiring relatively little energy.[21–23]

Our group has recently shown that nanoscale cuboctahedral Rhodium-based Metal-Organic Polyhedra (Rh-MOPs), a class of permanently porous metal-organic cages assembled from 24 (functionalised) 1,3-benzenedicarboxylate linkers and twelve dirhodium paddlewheels,[24] can also be harnessed for molecular separation, albeit through an alternative mechanism to host-guest recognition. Unlike other coordination cages, Rh-MOPs present twelve Rh(II) paddlewheels, each of which has an exohedral open metal site that can be used to bind molecules with coordinating groups (Figure 1).[25] This reactivity enables separation of physicochemically similar molecules that differ only in their affinity to the exposed Rh(II) axial sites of the Rh-MOP. For instance, we previously reported the utility of this reactivity in the separation of aliphatic and aromatic heterocycles that differ in their coordination affinity to Rh(II).[26]

Herein we report that steric hindrance in the coordination of the exohedral positions of Rh(II) ions in Rh-MOPs can efficiently drive the separation of pyridine regioisomeric mixtures, including a mixture of 2-ClPy and 3-ClPy (Figure 1). We determined, both experimentally and through simulations, that the capacity of pyridines to bind to the surface of Rh-MOPs is determined by the position of the pyridine substituents relative to the pyridine nitrogen. Accordingly, we reasoned that separation methodologies could be implemented based on the fact that the solubility of the bound pyridine-regioisomer is governed by the solubility of the Rh-MOP onto which it is anchored. Thus, we exploited the differential solubility of the coordinating and non- coordinating regioisomers to engineer liquid-liquid self-sorting systems. Using this method, we separated four different equimolecular mixtures of pyridine regioisomers, in all cases isolating the target compounds at a purity above 90%.

-Figure 1-

Results and Discussion

Selective coordination of Rh-MOPs to functionalised pyridines induced by steric hindrance: a mixture of lutidine regioisomers as a case study.

We chose a mixture of 2,6-lutidine and 3,5-lutidine as a model to study how substituent geometry influences the way that pyridines coordinate to the exposed axial sites of the dirhodium paddlewheels of Rh-MOPs. Thus, we tested the coordination capability of these two water-soluble regioisomers to an anionic cuboctahedral Rh-MOP of formula $Na_{24}[Rh_2(O\text{-}bdc)_2]_{12}$ (where O-bdc = 5-hydroxylate-1,3-benzenedicarboxylate; this MOP is hereafter named ONaRhMOP).[26] The aforementioned affinity of the dirhodium paddlewheel axial sites to N-donor ligands can be readily followed either by the naked eye or by monitoring spectroscopic changes in the bands centred in the range from 500 nm to 600 nm (λ_{max}), which corresponds to the $\pi^* \rightarrow \sigma^*$ transitions of Rh−Rh bonds.[27] Thus, we added 3,5-lutidine (12 mol. eq.) or 2,6-lutidine (12 mol. eq.) to an aqueous solution of ONaRhMOP (0.29 mM, pH = 11). Addition of 3,5-lutidine led to an immediate change in the colour of the ONaRhMOP solution, from green to purple, characteristically indicating coordination of the pyridine nitrogen to the dirhodium paddlewheel clusters.

Contrariwise, the addition of 2,6-lutidine did not induce any change in the colour of the ONaRhMOP solution, suggesting that the pyridine nitrogen in this compound cannot coordinate to said clusters. The corresponding UV-vis spectra confirmed these observations: when ONaRhMOP was treated with 3,5-lutidine (Figure 2a and S1), the λ_{max} shifted from 586 nm to 549 nm, whereas when it was treated with 2,6-lutidine, the λ_{max} (586 nm) did not change.

Next, we employed all-atomic Molecular Dynamics (MD) simulations in order to identify the mechanism responsible for the selective coordination observed experimentally. This was done by performing a series of simulations (Table S4) of atomistic models of ONaRhMOP and mixtures of 3,5-lutidine and 2,6-lutidine in solution. We employed NAMD,[28] VMD[29] and Gaussian 16[30] software for the simulations, as described in detail in the ESI.

In the first batch of simulations, we considered two different atomistic models of ONaRhMOP and 12 molecules of each species mixed in ⍰4000 water molecules at 298 K. Both ONaRhMOP models were based on the crystal structure of its protonated form (OHRhMOP), of formula [Rh2(OH-bdc)2]12 (where OH-bdc = 5-hydroxy-1,3 benzenedicarboxylate). In the first model (System 1 in Table S4), we considered the positions of the atoms involved in the dirhodium paddlewheel (i.e. Rh-O coordination bond and Rh-Rh bond) fixed to match those observed in the crystal structure of OHRhMOP. In the second model (System 2 in Table S4), we fixed only the Rh-Rh bond, allowing thermal distortions of the paddlewheel cluster in solution.

-Figure 2-

Crucially, the results of System 1 simulations did not show any selective behaviour but System 2 simulations showed selective Rh-N coordination of the ONaRhMOP toward 3,5-lutidine. In the simulations of System 1 (Figures S7-S9), 2,6-lutidine was found to bind perfectly to both the exohedral and endohedral axial sites of the dirhodium paddlewheel. On the contrary, the results of System 2 simulations generated a spontaneously distorted paddlewheel cluster in water. Note that the degree of distortion of this simulated paddlewheel was found to be within the range of experimentally observed distorted paddlewheel structures (Figure S10).[31] The distorted paddlewheel permits Rh-N coordination with 3,5-lutidine and inhibits Rh-N coordination to 2,6-lutidine, as we had observed experimentally (Figure 2b and Figure S11 - S14). Therefore, our MD simulation results predict that the crystal structure of OHRhMOP must be allowed to deform to show regioisomer selectivity. This prediction from simulations is experimentally supported by the fact that crystalline structures of rhodium acetate complex (Rh2(acetate)4) coordinated to 2,6-lutidines can be found in the literature.[32,33] This result suggested to us that, in the case of symmetric dirhodium paddlewheel clusters with reduced mobility, as in crystalline solids, there is no steric hindrance-driven selectivity for specific lutidine isomers. To further confirm this behaviour, we exposed ONaRhMOP crystals to 2,6-lutidine vapours. We observed that the sample turned purple within 12 hours, indicating that 2,6-lutidine does indeed coordinate to solid-state ONaRhMOP (Figure S2). Therefore, our MD simulations and the experimental evidence demonstrated that the dynamics of the ONaRhMOP in solution directs the selective coordination of this MOP toward 3,5-lutidine.

Detailed analysis of System 2 simulations revealed interesting molecular scale details of the interaction between ONaRhMOP and 3,5-lutidine or 2,6-lutidine. Our results showed that 3,5-lutidine preferentially coordinate to the exohedral axial site of the dirhodium paddlewheel clusters. The majority of the exohedral axial sites coordinate to one molecule of 3,5-lutidine; however, we found that 17% of them simultaneously coordinate to two 3,5-lutidine molecules (Figure S14). Additionally, we found that the

hydrophobic interactions of 3,5-lutidine with the squared windows of the ONaRhMOP enable this compound to enter the cavity of the MOP and subsequently coordinate to the endohedral axial site of the Rh-Rh paddlewheel (Figure S14). We have performed extensive molecular dynamics free-energy calculations using the adaptive biased force (ABF)[34] method in order to compare the free energy associated to the different coordination or adsorption modes (see Figures S15-S18 for the detailed calculations with their configurations). Our results showed that the most favourable coordination mode is a single 3,5-lutidine molecule coordinated to one external Rh(II) site with ΔG = -43.54 Kcal/mol (this is the configuration shown in the inset of Figure 2b). The free energy for the case of two molecules of 3,5-lutidine bound to one exohedral axial site was -31.76 Kcal/mol, whereas for the case of one molecule of 3,5-lutidine bound to each Rh(II) axial site of the paddlewheel, the value was -40.00 Kcal/mol. The only interaction observed between 2,6-lutidine and ONaRhMOP in our simulations were short lived contacts through π-π interactions, as illustrated in Figure 2b, which have ΔG = -6.06 Kcal/mol.

To corroborate the different coordination modes suggested by our computational simulations, we sought experimental evidence by analysing the UV-Vis spectra of ONaRhMOP that we had titrated with 3,5-lutidine. We observed that, after addition of 6 mol. eq. of 3,5-lutidine, the isosbestic point disappeared, indicating that not all Rh-Rh paddlewheels are coordinating to only one 3,5-lutidine molecule but that there is a portion of them that coordinate to two molecules of 3,5-lutidine (Figure S28 and S29).[35] The ^{1}H-NMR spectra of ONaRhMOP titrated with 2,6-lutidine revealed an upfield shift in the signals of all the lutidine protons, thereby providing experimental evidence of non-coordinative interactions between it and ONaRhMOP (Figure S35 and S36).

To further study the consistency between our MD simulation results and our experimental data, we performed additional MD simulations of a model identical to System 2 with only six molecules of each regioisomer per ONaRhMOP (System 3). This corresponds to the experimental conditions in which the isosbestic point is preserved during the titration. In this simulation, ONaRhMOP exhibited 100% coordination selectivity for 3,5-lutidine and, it only interacted with 2,6-lutidine through π-π stacking with its windows (Figure S20 - S22). These results indicated that 2,6-lutidine does not coordinate to ONaRhMOP, despite the presence of multiple free Rh-Rh axial sites. Additionally, we only observed one coordination mode of 3,5-lutidine to the dirhodium axial sites, which agrees with the maintenance of the isosbestic point upon addition of up to 6 mol. eq. of this regioisomer. Finally, we performed simulations of a much diluted system (System 4), build from System 2 with 12 molecules of each ligand but adding a much larger amount of water (~38000 water molecules instead of ~4000). This corresponds to a concentration of 1.47 mM, exactly corresponding to the experimental concentration used for separation experiments (*vide infra*). After equilibration for a very long time (~1 μs which is in the limit of timescales of MD simulations), we obtain again the same results (Figure S23- S27). The ensemble of experimental and computational results led us to conclude that ONaRhMOP in solution interacts differently with lutidine regioisomers in function of the position of the lutidine methyl groups.

Coordination-driven separation of lutidine regioisomers.

-Figure 3-

Having observed the regioisomeric preference of ONaRhMOP for coordination to 3,5-lutidine, relative to 2,6-lutidine, we envisaged that the difference in the type and strength of interaction between it and these two regioisomers could be exploited to achieve chemical separation by liquid-liquid extraction. To this end, we designed a separation protocol based on the premise that the solubility of the coordinated

pyridine would be dictated by the solubility of the ONaRhMOP. Thus, by taking advantage of the broad solubility profile of lutidines, the non-coordinated lutidine would be selectively extracted with an organic solvent, whereas the coordinated lutidine would remain attached to the ONaRhMOP in the aqueous phase (Figure 3a).

To test the separation of 2,6-lutidine and 3,5-lutidine mixtures enabled by ONaRhMOP, we first added 6 mol. eq. of each lutidine to an aqueous solution of ONaRhMOP (1.47 mM, pH = 11). We selected this stoichiometry because theoretical and experimental studies showed that, under these experimental conditions, each 3,5-lutidine coordinates preferentially to one axial site. This scenario maximizes the energy difference of the interaction of the ONaRhMOP with 3,5-lutidine relative to 2,6-lutidine. Once the regioisomer mixture was added, the solution immediately became purple (λ_{max} = 563 nm) (Figure S41), due to formation of the ONaRhMOP bound to 3,5-lutidine (hereafter named as ONaRhMOP(3,5-lutidine)). Then, cyclohexane was layered on top of the aforementioned solution and the biphasic system was shaken for 5 s to induce the extraction of 2,6-lutidine (Figure 3b). The ^{1}H-NMR spectra of the aqueous and the cyclohexane phases revealed that 2,6-lutidine had been completely removed from the aqueous phase after three consecutive extractions with fresh cyclohexane (Figure S39 and S40). Next, UV-Vis analysis of the aqueous phase confirmed that 3,5-lutidine had not detached from the ONaRhMOP during extraction process, as the λ_{max} remained at 563 nm throughout the process (Figure S41). Consistent with these observations, blank experiments performed without ONaRhMOP showed that 3,5-lutidine was partitioned between the organic and aqueous phase (Figures S37 and S38). Altogether, these results demonstrated that ONaRhMOP can retain a coordinating pyridine within one solvent, even if that pyridine is exposed to another solvent in which it is also soluble.

Next, we explored the release of 3,5-lutidine and subsequent recovery of the ONaRhMOP. For this, we used acetonitrile as a coordinating solvent to release 3,5-lutidine from ONaRhMOP via ligand exchange. Due to the solubility of 3,5-lutidine in water, we reasoned that its recovery from the aqueous phase would entail multiple extraction cycles with an organic solvent. Accordingly, we developed an alternative process that comprised first precipitating the ONaRhMOP(3,5-lutidine) complex via addition of BaCl2 to trigger a cationic exchange with Na(I) ions, rendering an insoluble salt (Figure S42). After removing the aqueous supernatant, the next step was addition of acetonitrile-d_3 to the solid to detach 3,5-lutidine from the precipitated salt. The 1H-NMR spectrum of the acetonitrile- d_3 revealed the presence of pure 3,5-lutidine (Figure 3c and Figure S43). Next, ONaRhMOP was recovered by first adding HCl to the solid from the previous step, to yield OHRhMOP, which was finally converted into ONaRhMOP upon addition of NaOH (Figure 3a). Overall, this liquid-liquid extraction process enabled us to obtain pure lutidine regioisomers from equimolar mixtures. Moreover, the integrity of the ONaRhMOP was maintained through the whole cycle, as evidenced by UV-Vis, ^{1}H-NMR and Mass Spectrometry measurements (Figures S44 - S46).

Expanding the scope: separation of 2- and 4-monosubstituted pyridines.

-Figure 4-

Encouraged by our previous results, we sought to use Rh-MOP to separate regioisomers of monosubstituted pyridines, which exhibit less steric hindrance around the coordinating heteroatom than do the corresponding disubstituted pyridines. Accordingly, we evaluated the feasibility of using Rh-MOPs to separate two regioisomeric mixtures of 2- and 4-substituted pyridine moieties. As model systems, we selected regioisomeric mixtures of pyridines functionalised with carboxylic acid groups or halogen atoms. For each mixture, we established a working protocol. Firstly, we determined the selective coordination of

the Rh-MOP core toward one of the regioisomers in solution. Secondly, we implemented this selective interaction in a biphasic liquid-liquid extraction system by considering the solubility profiles in each regioisomeric mixture.

Thus, we first titrated OHRhMOP (0.29 mM) with solutions of picolinic acid (2-COOHPy) in methanol and of isonicotinic acid (4-COOHPy) in methanol/DMF (1:1). Next, we performed a similar experiment using solutions of 2-iodopyridine (2-IPy) and of 4- iodopyridine (4-IPy), both in DMF/methanol (1:1). The UV-Vis spectra revealed that in both experiments, the OHRhMOP had selectively coordinated to the corresponding 4-substituted pyridine (Figure S47 and S48).

The two regioisomeric mixtures that we tested show a clear preference for either hydrophobic (4/2-IPy) or hydrophilic (4/2-COOHPy) solvents, thereby complicating use of the selective retention strategy that we had earlier used to separate the lutidines. Thus, we decided to implement a biphasic extraction approach, whereby the Rh-MOP acts as a selective extracting agent for the 4-substituted pyridine. This approach entails coordination of the 4-substituted pyridine to the Rh-MOP in situ, at the interface of two immiscible liquids, and its subsequent transfer to the solution containing the Rh-MOP.

In the case of hydrophobic 2-IPy and 4-IPy, we designed an extraction system in which the extracting Rh-MOP was in the aqueous phase, whereas the regioisomeric mixture was dissolved in an organic solvent. To this end, we prepared a biphasic system comprising a toluene phase, containing an equimolar mixture of 4-IPy and 2-IPy (17.64 mM, 12 mol. eq. per MOP), layered on top of an aqueous phase, containing ONaRhMOP (1.47 mM, pH = 11) (Figure 4a). The ^{1}H-NMR spectrum of the toluene phase obtained after shaking the biphasic system for 5 s revealed the presence of pure 2-IPy (Figures 4b and S51). The UV-Vis spectrum of the aqueous phase showed the expected shift of λ_{max} from 585 nm to 549 nm, corroborating the coordination of ONaRhMOP to 12 molecules of 4-IPy (Figure S50). The 4-IPy was then recovered in a fresh toluene phase, by adding 10 µL of acetonitrile to the aqueous phase and shaking the biphasic system for 5 s. Acetonitrile triggered the release of 4-IPy from ONaRhMOP through a ligand-exchange mechanism. Upon shaking of the biphasic system, the 4-IPy rapidly migrated into the toluene phase, as it is insoluble in water. The ^{1}H-NMR spectrum of the toluene phase indicated recovery of pure 4-IPy (Figures 4b and S52). The acetonitrile was easily removed from the aqueous phase by washing it with chloroform, enabling recovery of pure ONaRhMOP, with no traces of acetonitrile and no sign of degradation over the separation cycle (Figures S53- S55).

-Figure 5-

Both 2-COOHPy and 4-COOHPy are highly soluble in water, but they are not soluble in other water-immiscible organic solvents. Accordingly, we decided to implement an extraction approach whereby the Rh-MOP acts as an extracting agent in the organic phase. Thus, we selected a hydrophobic Rh-MOP of formula $[Rh_2(C_{12}\text{-bdc})_2]_{12}$ (where *C_{12}-bdc* = dodecoxybenzene-1,3-dicarboxylate; this MOP is hereafter called *C_{12}RhMOP*), whose surface is functionalised with 24 aliphatic chains.[36] Despite this hydrophobic functionalisation, C_{12}RhMOP also showed coordination selectivity for 4-COOHPy over 2-COOHPy in solution, as determined by UV-Vis experiments done in DMF (Figure S57). Next, we prepared a biphasic system of a solution of 4-COOHPy and 2-COOHPy (both at 11.16 mM, 12 mol. eq. per MOP) in water and C_{12}RhMOP (0.93 mM) in chloroform (Figure 5). After the biphasic system had been shaken for 5s, the two different phases were separately analysed. The UV-Vis spectrum of the chloroform phase showed a λ_{max} of 544 nm, indicative of the coordination of 12 molecules of 4-COOHPy to C_{12}RhMOP, suggesting complete

separation of the two regioisomers (Figure S57). The 1H-NMR of the water phase corroborated this observation, as 2-COOHPy was found to be pure after the liquid-liquid extraction (Figure 5 and S58).

Next, we employed a pH-triggered release of bound 4-COOHPy, by layering a dilute aqueous acid solution (0.3 M HCl) on top of the chloroform phase (Figure 5). Note that we did not use acetonitrile to release 4-COOHPy, because it would have been difficult to remove it from the chloroform phase after the separation cycle, thus hindering the recovery of the C_{12}RhMOP. Shaking of the biphasic system for 15 s induced a change in colour of the chloroform phase, from purple to green, which was characterised by UV-Vis spectroscopy, which revealed a shift of λ_{max} from 544 nm to 627 nm, indicative of the detachment of 4-COOHPy from C_{12}RhMOP (Figure S60). The ^{1}H-NMR spectra of the two phases revealed that the aqueous phase contained 4-COOHPy (Figure 5 and S59), whereas the organic phase contained the recovered C_{12}RhMOP (Figure S61). The integrity of the C_{12}RhMOP had been maintained throughout the separation cycle, as evidenced by UV-Vis, ^{1}H-NMR and Mass Spectrometry (Figures S60- S62).

Separation of an industrially relevant mixture: 2-chloropyridine/3-chloropyridine

Having demonstrated the feasibility of separating pyridinic regioisomers, we next sought to apply our liquid-liquid extraction system to separate an industrially relevant isomeric pyridine mixture. Monosubstituted chloropyridines, and especially 2-ClPy, are frequently used as synthetic intermediates in many sectors, such as pharmaceuticals, pesticides and fine chemicals.[37] However, the synthesis of 2-ClPy is generally not selective, producing the isomer 3-ClPy as a by-product. Thus, major efforts have recently been devoted to optimising the separation of 2-ClPy and 3-ClPy, which is currently based on the high energy demanding distillation method (boiling point of 2-ClPy and 3-ClPy is 166ºC and 148ºC, respectively).[38] For this reason, we considered the mixture an ideal model system on which to test our methodology. To target this separation, we first tested the selectivity of our model OHRhMOP core for 3-ClPy (over 2-ClPy), through UV-Vis analysis of the solutions obtained after titrating OHRhMOP (0.29 mM) with 12 mol. eq. of 3-ClPy or 2-ClPy in methanol/DMF (1:1). In these tests, we only observed a shift in λmax for those solutions titrated with 3-ClPy, which indicated that the steric hindrance-driven coordination selectivity also applies in this case, despite the small size and vicinity of the pyridine substituents (Figure S63). Inspired by this result, we designed a liquid-liquid extraction system based on the solubility and hydrophobic character of 3-ClPy and 2-ClPy. To this end, we prepared a water-cyclohexane biphasic system in which both pyridine regioisomers were dissolved in the organic phase at 8.82 mM (6 mol. eq. per Rh-MOP), and in which ONaRhMOP (1.47 mM, pH = 11) was dissolved in the aqueous phase (Figure 6). Shaking of this biphasic system for 5 s resulted in an immediate change in the colour of the aqueous phase, from green to purple. Spectroscopic characterisation revealed the presence of pure 2-ClPy in the cyclohexane phase, whereas 3-ClPy was coordinated to ONaRhMOP and transferred to the aqueous phase (Figure 6 and Figure S65 and S66). The fact that 3-ClPy is also soluble in chloroform enabled us to recover it as a pure fraction upon addition of acetonitrile to a water-chloroform biphasic system (Figure S67). Moreover, this configuration allowed us to remove acetonitrile from the aqueous phase and therefore, to recover the initial ONaRhMOP in its active form for further use (Figure S69). The ease of recovering ONaRhMOP after the separation of 3-ClPy and 2-ClPy prompted us to perform several extraction cycles to separate regioisomeric mixtures at a higher concentration (70.6 mM, 48 mol. eq. per Rh-MOP). We found that, after six extraction cycles, 3-ClPy was completely removed from the initial equimolar mixture; thus, we obtained pure 2-ClPy in the cyclohexane phase (Figure S68). Additionally, Mass Spectrometry and 1H-NMR confirmed the integrity of the ONaRhMOP after the extraction cycles (Figures S70, S71).

-Figure 6-

Conclusion

We have demonstrated that Rh(II)-MOP can be harnessed for use in a liquid-liquid extraction system to separate regioisomers of substituted pyridines. We found that steric hindrance from the pyridine substituents surrounding the coordinating N-atom leads to selectivity in the exohedral coordination positions of the dirhodium paddlewheels in solution. To elucidate this mechanism, we combined computational and experimental studies, including large-scale all atomic MD simulations of systems of up to ⍰ 105 atoms up to time scales of ⍰ 1 μs. We exploited this phenomenon to obtain pure phases of four different regioisomeric mixtures of pyridines of diverse physicochemical properties and degrees of steric hindrance. We validated our system by using two different approaches: using the Rh(II)-MOP as retaining agent or as extracting agent. Such versatility, combined with the tuneable solubility provided by external organic functionalisation of Rh(II)-MOP, enabled us to adapt our extraction system to the specifics of each isomeric mixture. We believe that this steric hindrance-driven selectivity will open up new avenues in the field of chemical purifications, including for challenging mixtures such as racemates, as well as for practical applications such as pollutant removal and drug purification.

Acknowledgements

This work was supported by the Spanish MINECO (project RTI2018-095622-B-I00) and the Catalan AGAUR (project 2017 SGR 238). It was also funded by the CERCA Programme /Generalitat de Catalunya. ICN2 is supported by the Severo Ochoa programme from the Spanish MINECO (Grant No. SEV-2017-0706). A.C.S. and T.G. thank the Spanish MINECO for Juan de la Cierva fellowships (IJCI-2016-29802 and FJCI-2017-31598). F.G. acknowledges funding from the Spanish Research Agency (AEI, CTQ2017-87262-R, EUR2019-103824). The project that generated these results received support from a fellowship (LCF/BQ/PR20/11770011) of the ”la Caixa” Foundation (ID 100010434).

Keywords: Metal-organic polyhedra • separation • regioisomers • liquid-liquid extraction • steric hindrance

[1] S.S. David, R. P. Lively, Nature. 2016, 532, 435–437.

[2] Materials for Separation Technologies. Energy and Emission Reduction Opportunities, United States, 2005.

[3] R. A. Meyers, Handbook of Petroleum Refining Processes, Third Edition, McGraw-Hill Education, New York, 2004.

[4] Y. Yang, P. Bai, X. Guo, Ind. Eng. Chem. Res. 2017, 56, 14725–14753.

[5] W. B. Wilson, L. C. Sander, M. L. de Alda, M. L. Lee, S. A. Wise, J. Chromatogr. A 2016, 1461, 107–119.

[6] M. P. Marszałł, M. J. Markuszewski, R. Kaliszan, J. Pharm. Biomed. Anal. 2006, 41, 329–332.

[7] M. C. Hilton, R. D. Dolewski, A. McNally, J. Am. Chem. Soc. 2016, 138, 13806–13809.

[8] S. Shimizu, N. Watanabe, T. Kataoka, T. Shoji, N. Abe, S. Morishita, H. Ichimura, Ullmann's Encycl. Ind. Chem. 2000.

[9] S. V Sivakumar, D. P. Rao, Chem. Eng. Process. Process Intensif. 2012, 53, 31–52.

[10] X. Gu, J. Dong, T. M. Nenoff, D. E. Ozokwelu, J. Memb. Sci. 2006, 280, 624–633.

[11] J. Huang, X. Han, S. Yang, Y. Cao, C. Yuan, Y. Liu, J. Wang, Y. Cui, J. Am. Chem. Soc. 2019, 141, 8996–9003.

[12] Z. R. Herm, B. M. Wiers, J. A. Mason, J. M. van Baten, M. R. Hudson, P. Zajdel, C. M. Brown, N. Masciocchi, R. Krishna, J. R. Long, Science 2013, 340, 960-964.

[13] Z.-Y. Gu, D.-Q. Jiang, H.-F. Wang, X.-Y. Cui, X.-P. Yan, J. Phys. Chem. C 2010, 114, 311–316.

[14] D.-S. Guo, Y. Liu, Chem. Soc. Rev. 2012, 41, 5907–5921.

[15] T. Ogoshi, K. Kitajima, T. Aoki, T. Yamagishi, Y. Nakamoto, J. Phys. Chem. Lett. 2010, 1, 817–821.

[16] T. Tozawa, J. T. A. Jones, S. I. Swamy, S. Jiang, D. J. Adams, S. Shakespeare, R. Clowes, D. Bradshaw, T. Hasell, S. Y. Chong, C. Tang, S. Thompson, J. Parker, A. Trewin, J. Bacsa, A. M. Z. Slawin, A. Steiner, A. I. Cooper, Nat. Mater. 2009, 8, 973–978.

[17] D. Zhang, T. K. Ronson, J. R. Nitschke, Acc. Chem. Res. 2018, 51, 2423–2436.

[18] T. R. Cook, P. J. Stang, Chem. Rev. 2015, 115, 7001–7045.

[19] D. Fujita, Y. Ueda, S. Sato, N. Mizuno, T. Kumasaka, M. Fujita, Nature 2016, 540, 563–566.

[20] G. Liu, Y. Di Yuan, J. Wang, Y. Cheng, S. B. Peh, Y. Wang, Y. Qian, J. Dong, D. Yuan, D. Zhao, J. Am. Chem. Soc. 2018, 140, 6231.

[21] G. Zhang, A.-H. Emwas, U. F. Shahul Hameed, S. T. Arold, P. Yang, A. Chen, J.-F. Xiang, N. M. Khashab, Chem 2020, 6, 1082–1096.

[22] J. Hu, J. S. Ward, A. Chaumont, K. Rissanen, J.-M. Vincent, V. Heitz, H.-P. Jacquot de Rouville, Angew. Chem. Int. Ed. 2020, 59, 23206.

[23] D. Zhang, T. K. Ronson, R. Lavendomme, J. R. Nitschke, J. Am. Chem. Soc. 2019, 141, 18949–18953.

[24] S. Furukawa, N. Horike, M. Kondo, Y. Hijikata, A. Carné-Sánchez, P. Larpent, N. Louvain, S. Diring, H. Sato, R. Matsuda, R. Kawano, S. Kitagawa, Inorg. Chem. 2016, 55, 10843–10846.

[25] A. Carné-Sánchez, J. Albalad, T. Grancha, I. Imaz, J. Juanhuix, P. Larpent, S. Furukawa, D. Maspoch, J. Am. Chem. Soc. 2019, 141, 4094–4102.

[26] T. Grancha, A. Carné-Sánchez, L. Hernández-López, J. Albalad, I. Imaz, J. Juanhuix, D. Maspoch, J. Am. Chem. Soc. 2019, 141, 18349–18355.

[27] E. B. Boyar, S. D. Robinson, Coord. Chem. Rev. 1983, 50, 109–208.

[28] J. C. Phillips, R. Braun, W. Wang, J. Gumbart, E. Tajkhorshid, E. Villa, C. Chipot, R. D. Skeel, L. Kalé, K. Schulten, J. Comput Chem. 2005, 26, 1781−1802

[29] W. Humphrey, A. Dalke, K. Schulten, J. Mol. Graphics 1996, 14, 33.

[30] M. J. Frisch, G. W. Trucks, H. B. Schlegel, et al., Gaussian 16, Revision A.03, Gaussian, Inc., Wallingford CT, 2016.

[31] F. Haase., G. A. Craig, Bonneau, M. K. Suguimoto, Furukawa, S. J. Am. Chem. Soc. Rev. 2020, 142, 13839.

[32] E. Warzecha, T. C. Berto, J. F. Berry, Inorg. Chem. 2015, 54, 8817–8824.

[33] K. Aoki, M. Inaba, S. Teratani, H. Yamazaki, Y. Miyashita, Inorg. Chem. 1994, 33, 3018–3020.

[34] J. Henin, G. Fiorin, C. Chipot, M. L. Klein, J. Chem. Theory Comput. 2010, 6, 35- 47.

[35] X. Xu, M. P. Doyle, Inorg. Chem. 2011, 50, 7610.

[36] K. Kawano, N. Horike, Y. Hijikata, M. Kondo, A. Carné-Sánchez, P. Larpent, S. Ikemura, T. Osaki, K. Kamiya, S. Kitagawa, S. Takeuchi, S. Furukawa, Chem. 2017, 2, 393-403.

[37] C. Skoutelis, M. Antonopoulou, I. Konstantinou, D. Vlastos, M. Papadaki, J. Hazard. Mater. 2017, 321, 753–763.

[38] X. Sheng, E. Li, Y. Zhou, R. Zhao, W. Zhu, F. Huang, J. Am. Chem. Soc. 2020, 142, 6360–6364.

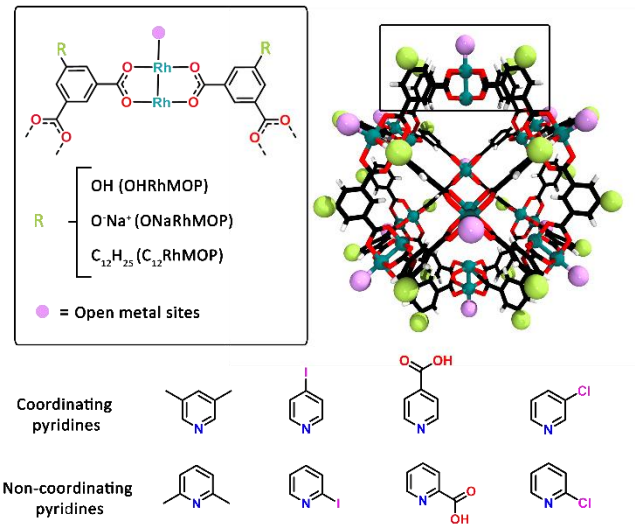

Figure 1. Top: Structure of cuboctahedral Rh-MOP, highlighting the axial sites of its dirhodium paddlewheels. Bottom: Chemical structures of the coordinating and non-coordinating pyridine-based regioisomers separated in this study.

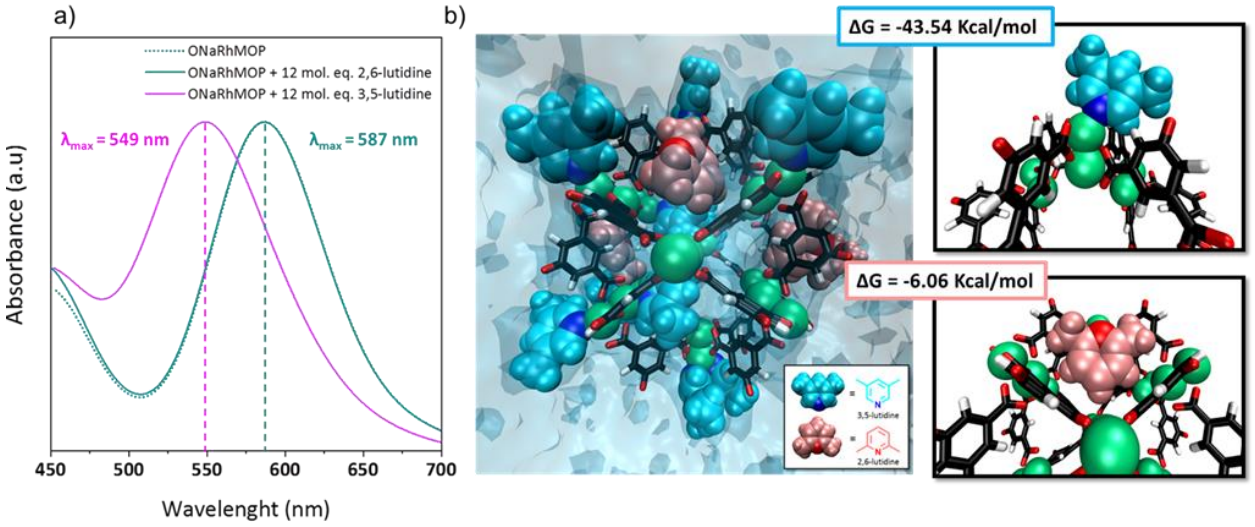

Figure 2. (a) UV-Vis spectra of ONaRhMOP in water before (turquoise) and after (pink) addition of 12 mol. eq. of 3,5-lutidine. (b) Screenshot of an instantaneous configuration obtained during a Molecular Dynamics simulation of a system with one ONaRhMOP and a 1:1 mixture of 3,5-lutidine and 2,6-lutidine molecules in water (12 ligand molecules of each species, System 2 of Table S4). The ONaRhMOP is shown in licorice representation with the Rh atoms emphasized as green Van der Waals spheres. We show the closest 2,6-lutidine molecules (pink color) and all 3,5-lutidine (cyan color) molecules with their N atom emphasized. Water molecules are not shown for clarity. In this image we observe Rh-N coordination between ONaRhMOP and all 3,5-lutidine molecules. Several 2,6-lutidine molecules can be observed near the ONaRhMOP with three of them making short-lived contacts. Insets: detailed images of the stable adsorption site of 3,5-lutidine with Rh-N coordination at the axial site of a dirhodium paddlewheel (top right), and of a configuration corresponding to a short lived contact of 2,6-lutidine with the squared window of the ONaRhMOP through a π-π interaction between (bottom right). The free energy corresponding to each interaction calculated from ABF-MD simulations is also shown (see main text for details).

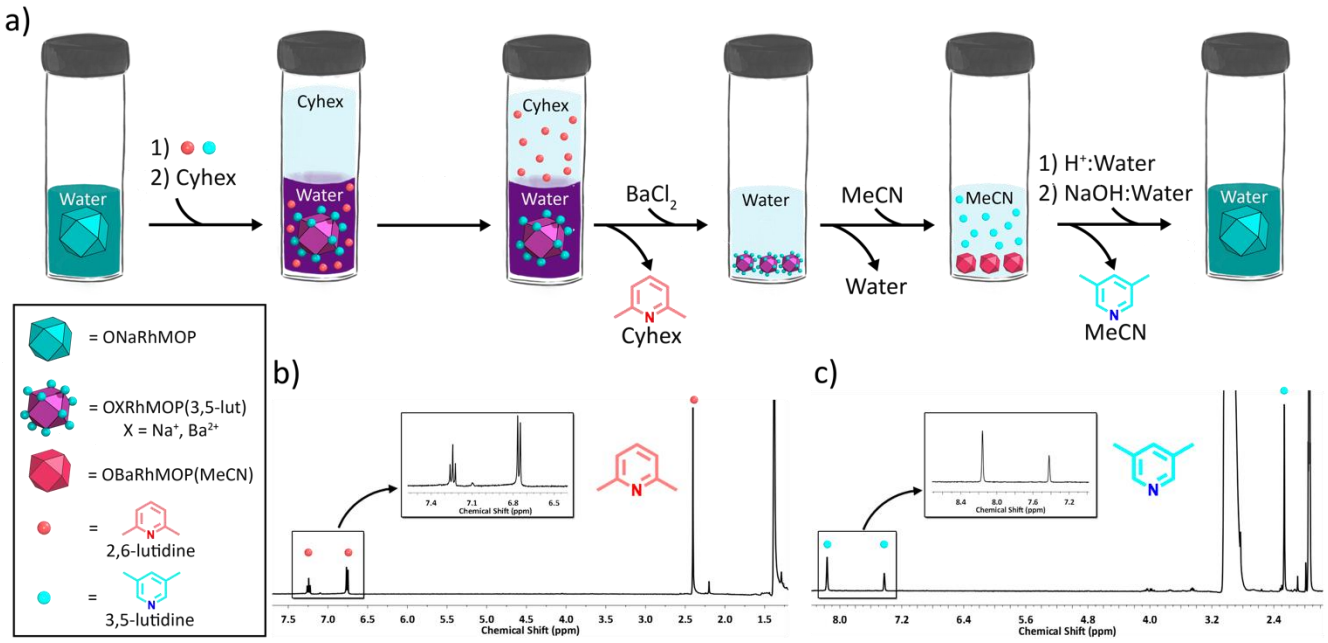

Figure 3. (a) Schematic of the selective retention of 3,5-lutidine in water and its subsequent recovery in acetonitrile. (b) ^{1}H-NMR spectrum of 2,6-lutidine in cyclohexane-d_{12} (Cyhex). (c) ^{1}H-NMR spectrum of 3,5-lutidine in acetonitrile-d_3 (MeCN).

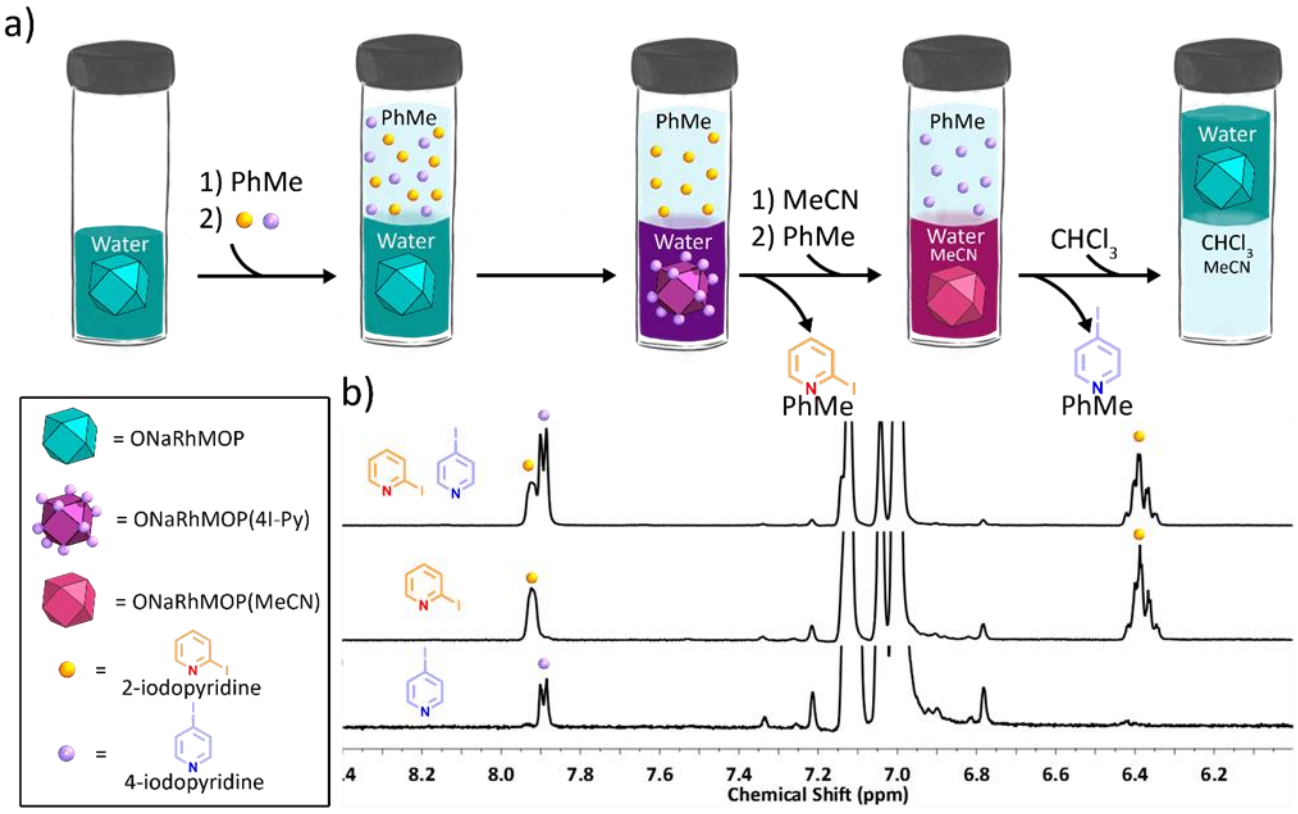

Figure 4. (a) Schematic representation of the selective biphasic extraction of 4-IPy into the aqueous phase and the subsequent recovery of the ONaRhMOP. (b) Stacked ^{1}H-NMR spectra of the toluene-d_8 phase before the extraction (top), after the first extraction (middle), and after the recovery of 4-IPy (bottom)

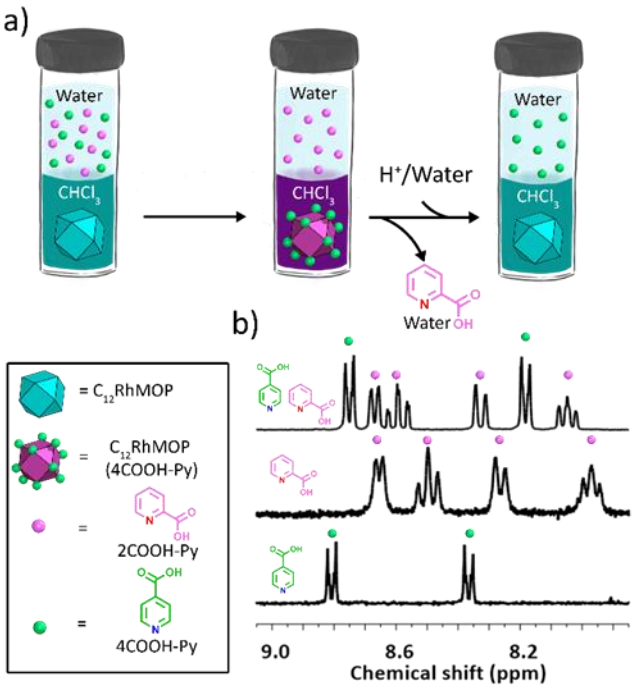

Figure 5. (a) Schematic representation of the selective liquid-liquid extraction of 4-COOH-Py into the chloroform phase and its subsequent recovery in the aqueous phase. (b) Stacked ^{1}H-NMR spectra of the D_2O phase before the extraction (top), after the extraction (middle), and after the recovery of 4-COOH-Py (bottom).

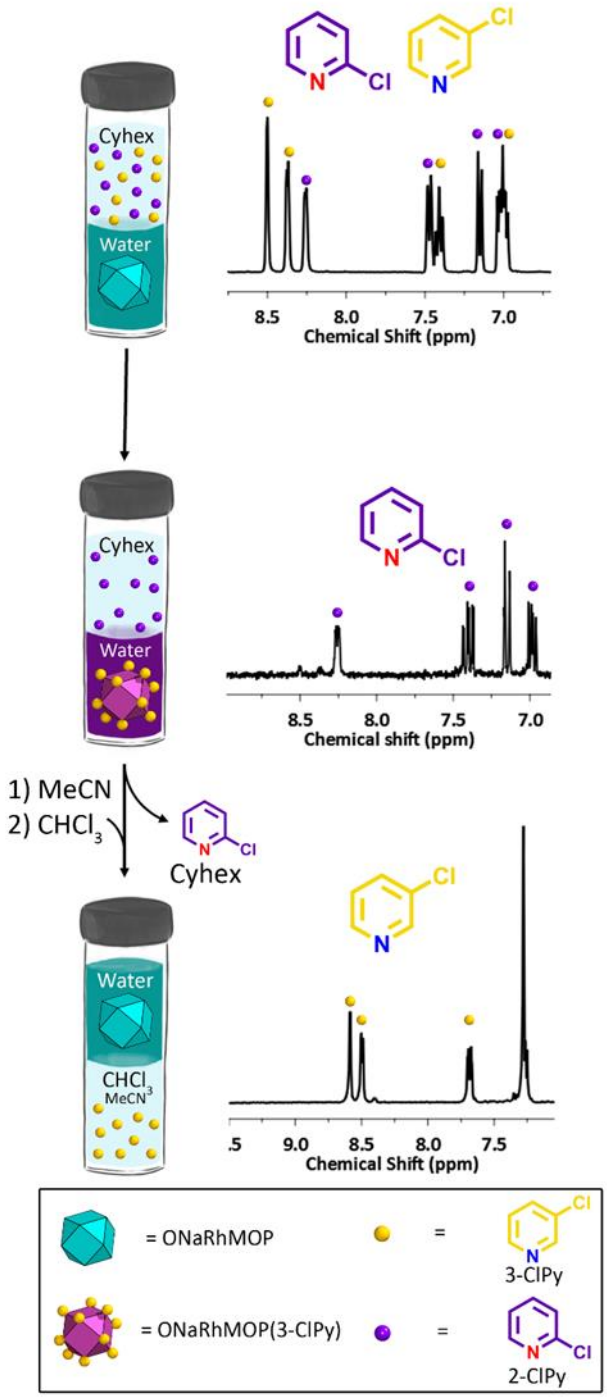

Figure 6. Schematic representation of the selective extraction of 3-ClPy from cyclohexane-d_8, and its subsequent recovery in $CDCl_3$ (left); and the corresponding 1H NMR spectra after each separation step (right).